HHS Public Access

Author manuscript

Sci Transl Med. Author manuscript; available in PMC 2021 November 28.

Published in final edited form as:

Sci Transl Med. 2021 January 13; 13(576): . doi:10.1126/scitranslmed.aaz1458.

Kidney disease genetic risk variants alter lysosomal beta-mannosidase (*MANBA*) expression and disease severity

Xiangchen Gu[2,3,*], **Hongliu Yang**[1,2,*], **Xin Sheng**[2,*], **Yi-An Ko**[2], **Chengxiang Qiu**[2], **Jihwan Park**[2], **Shizheng Huang**[2], **Rachel Kember**[4], **Renae L. Judy**[5], **Joseph Park**[4,10], **Scott M. Damrauer**[5,6], **Girish Nadkarni**[7,8,9], **Ruth JF Loos**[8], **Vy Thi Ha My**[8], **Kumardeep Chaudhary**[8], **Erwin P Bottinger**[8,9], **Ishan Paranjpe**[8], **Aparna Saha**[8], **Christopher Brown**[10], **Shreeram Akilesh**[11], **Adriana M. Hung**[12,13], **Matthew Palmer**[14], **Aris Baras**[15], **John D. Overton**[15], **Jeffrey Reid**[15], **Marylyn Ritchie**[4,10], **Daniel J. Rader**[2,4,10], **Katalin Susztak**[2,10]

[1]Division of Nephrology, West China Hospital of Sichuan University, Chengdu, China, 610041.

[2]Department of Medicine Perelman School of Medicine, University of Pennsylvania, PA, USA, 19104.

[3]Division of Nephrology, Yue Yang Hospital of Integrative Traditional Chinese and Western Medicine, Affiliated to Shanghai University of Traditional Chinese Medicine, Shanghai, China,200437.

[4]Institute for Translational Medicine and Therapeutics, University of Pennsylvania School of Medicine, PA, USA, 19104.

[5]Department of Surgery, University of Pennsylvania School of Medicine, PA, USA, 19104.

[6]Corporal Michael Crescenz VA Medical Center, Philadelphia, PA, USA, 19104.

[7]Division of Nephrology, Icahn School of Medicine at Mount Sinai, NY, USA, 10029.

[8]The Charles Bronfman Institute of Personalized Medicine, Icahn School of Medicine at Mount Sinai, NY, USA, 10029.

[9]The Hasso Plattner Institute of Digital Health, Icahn School of Medicine at Mount Sinai, NY, USA, 10029.

[10]Department of Genetics Perelman School of Medicine, University of Pennsylvania, PA, USA, 19104.

[11]Department of Pathology, University of Washington, Seattle, WA, USA, 98195.

[12]Nashville VA Medical Center, Nashville, TN, USA, 37212.

Correspondence: Katalin Susztak; ksusztak@pennmedicine.upenn.edu.

*These authors contributed equally

Author contributions: K.S. designed the study. X.G., H.Y., and S.H. conducted the experiments. X.S., Y.K., C.Q., and J.P. performed bioinformatic analyses. X.S., Y.K., R.K., R.L.J., J.P., M.R., S.M.D., and D.J.R. coordinated and managed genotype and phenotype data ascertainment in the Pennmedicine biobank. G.N., R.J.L., V.T.M., K.C., E.P.B., I.P., and A.S. coordinated and managed genotype and phenotype data ascertainment in the Biome biobank. S.A. performed Hi-C data analysis. M.P. evaluated the kidney histology. X.G., H.Y., and X.S. analyzed the data. K.S., X.G., and H.Y. wrote the manuscript. All authors helped to interpret results and approved the final version of the manuscript.

[13]Vanderbilt Center for Kidney Disease, Vanderbilt University Medical Center, Nashville, TN, USA, 37212.

[14]Department of Pathology and Laboratory Medicine, Perelman School of Medicine, University of Pennsylvania, PA, USA, 19104.

[15]Regeneron Genetics Center(RGC), 777 Old Saw Mill River Rd, Tarrytown, NY, USA,10591

Abstract

More than 800 million people in the world suffer from chronic kidney disease (CKD). Genome-wide association studies (GWAS) have identified hundreds of loci where genetic variants are associated with kidney function, however, causal genes and pathways for CKD remain unknown. Here we performed integration of kidney function GWAS studies and human kidney-specific expression quantitative trait analysis (eQTL) and identified that the expression of beta mannosidase (*MANBA*) was lower in kidneys of subjects with CKD risk genotype. We also show an increased incidence of renal failure in subjects with rare heterozygous loss of function coding variants in *MANBA* using phenome-wide association analysis (PheWAS) of 40,963 subjects with exome sequencing data. *MANBA* is a lysosomal gene highly expressed in kidney tubule cells. Deep phenotyping revealed structural and functional lysosomal alterations in human kidneys from subjects with CKD risk alleles and mice with genetic deletion of *Manba*. *Manba* heterozygous and knock-out mice developed more severe kidney fibrosis when subjected to toxic injury induced by cisplatin or folic acid. *Manba* loss altered multiple pathways, including endocytosis and autophagy. In the absence of *Manba*, toxic acute tubule injury induced inflammasome activation and fibrosis. Taken together, these results illustrate the convergence of common non-coding and rare coding variants in *MANBA* in kidney disease development and demonstrate the role of the endolysosomal system in kidney disease development.

One-sentence summary:

MANBA is a kidney disease risk gene that alters tubular endolysosomal function, inducing inflammasome activation and fibrosis.

INTRODUCTION

Chronic kidney disease (CKD) is a global public health burden affecting more than 800 million people worldwide (1). CKD is associated with complex metabolic disturbances, and markedly increased mortality. Diabetes, hypertension, old age, and toxic injury remain the key cause of CKD worldwide. Heritability of kidney function is estimated to be 30–50% (2).

Genome-wide association studies (GWAS) have emerged as an important method to map disease associated loci by testing the association of sequence variants across the genome with a disease or a trait of interest (3). The genetic underpinning of CKD has been analyzed by genotyping and phenotyping large numbers of subjects with varying degrees of kidney dysfunction(4, 5). Although GWAS has been highly effective in identifying genetic variations associated with disease states, these observations have not translated into better understanding of disease-causing genes, cell types, and mechanisms (6). A fundamental limitation has been that almost all disease-associated variants are located in the

non-coding region of the genome(7). The most widely accepted view is that disease-causing variants reside on cell-type specific regulatory regions (8) and the causal variant alters transcription factor binding strength, leading to quantitative differences in expression in cell-type specific target genes. To identify genes influenced by GWAS variants, the expression quantitative trait loci (eQTL) analysis has gained popularity, which defines the association between genetic variants and tissue gene expression(9). Integration of GWAS, eQTL, and epigenome annotation studies has been successfully used to identify disease-causing genes from GWAS studies(10). Our group has previously generated an eQTL atlas for the human kidney cortex and later microdissected glomerular and tubule compartments (5, 8). Computational integration of GWAS and eQTL datasets using Bayesian colocalization or Mendelian randomization methods highlighted 24 putative causal genes for kidney disease development (8). However, detailed *in vivo* and *in vitro* follow-up studies have been limited to a few loci. These studies identified *UMOD* on chromosome 16 and *DAB2* on chromosome 5 as disease-causing genes(8, 11). *DAB2* is expressed by proximal tubule cells. Genetic lowering of *Dab2* expression in kidney tubules protected mice from kidney injury. *In vitro* studies indicated that *Dab2* plays an important role in endocytosis. In this manuscript, we provide evidence that *MANBA* is a third kidney disease risk gene by computational integration of GWAS and eQTL studies, phenotype analysis of cohorts with exome-sequencing and mechanistic experiments using genetic knock-out mice and cells. Our mechanistic studies indicate that lower *Manba* expression leads to structural and functional lysosomal alterations, a block in endocytosis and autophagy, ultimately inducing an inflammatory cell death and fibrosis after an acute toxic injury.

RESULTS

Identification of *MANBA* as a CKD risk gene

Common non-coding nucleotide variations on chromosome 4 have been associated with kidney function (creatinine based estimated glomerular filtration rate [$eGFR_{crea}$] and blood urea nitrogen [BUN]) and CKD in multiple GWAS analyses (12–15). The GWAS association was initially reported in 2016 by the CKDGen consortium (4) and later replicated in a larger European and recently in a multi-ethnic cohort (Fig.1 and fig.S1)(12–14). The locus has been named based on its vicinity to *MANBA* and *NFKB1* (Fig.1, A and B). Annotation of this region with whole-kidney eQTL data indicated that variants in this region significantly (p=9.086e-5) influenced the expression of *MANBA* in human kidney cortex samples (Fig.1A). By examining association of the genotype and kidney function (in GWAS) and genotype and gene expression in a collection (n=150) microdissected human kidney tubule samples we found that multiple SNPs showed a strong association with *MANBA* and *CISD2* expression (top p-values 9.4e-6 and 4e-7, respectively) but not with *NFKB1* expression (Fig.1, A and B and fig. S2). The genotype-gene expression association of the top GWAS variants and MANBA expression in microdissected glomerular and tubule samples was significant (P=3.55E-6 in glomeruli and P=9.39E-6 in tubules, respectively (fig. S3). Furthermore, we also found a nominally significant SNP-gene expression association (P=0.027 in Glomeruli and 0.047 in tubule) in a publicly available human kidney eQTL database (generated from diseased kidney tissue samples) (10) (fig.S4). Examining the genotype-expression correlation in the GTEx compendium (9), we detected an association

between the CKD risk genotype and *MANBA* expression in multiple tissue types (p=4E-82 in GTEx multi-tissue eQTL) (fig.S5 and S6). We did not observe an association between this genetic variant and expression of *NFKB1* in kidney, liver, or blood samples (fig.S3 to S6).

Next, we performed Bayesian colocalization studies at this locus to understand whether the genetic variants that control *MANBA* expression and kidney disease risk originate from the same region. We found evidence for significant colocalization (PP4=0.99) between kidney disease-associated variants and variants associated with *MANBA* and *CISD2* expression in kidney tubule samples (Fig.1, A and B) (16). Again, we failed to see an association between disease risk variants and *NFKB1* expression (fig.S2).

Furthermore, analyzing human kidney chromatin conformation capture data (Hi-C) we confirmed that the GWAS variants are in physical contact with numerous accessible chromatin regions that overlap with DNase I-hypersensitive sites at the *MANBA* promoter and gene body (fig. S7), further supporting that *MANBA* is the target gene of the risk variants.

In summary, by analyzing multiple kidney disease GWASs and human kidney eQTLs, we demonstrate that variants identified in kidney function GWAS are associated with *MANBA* expression in human kidney tubule samples.

Individuals with heterozygous loss of function variants in *MANBA* have increased incidence of renal failure

Integration of GWAS and eQTL indicated that common non-coding variants on chromosome 4 are associated with kidney function and lower *MANBA* expression in kidney tubules. We next analyzed the association between rare protein altering loss-of-function (LoF) coding variants of *MANBA* and kidney phenotypes in two large cohorts; the PennMedicine BioBank (PMBB) and the BioMe Biobank. PMBB had 9,713 subjects with clinical and exome sequencing data, whereas 31,250 subjects with clinical and whole exome sequencing data were available in the BioMe biobank. We were not able to identify subjects with homozygous LoF variants, but we identified 11 heterozygous LoF variants in PMBB and 35 in BioMe. For unbiased phenotype ascertainment we performed phenome-wide association analysis (PheWAS) by comparing diagnostic code-based disease phenotypes (ICD9) in cases (heterozygous LoF) and controls in these large biobanks (fig.S8). The incidence of neuropsychiatric and respiratory diseases was higher amongst the *MANBA* het LoFs (fig.S8). This finding was consistent with the disease spectrum already reported for subjects with homozygous LoF (17). By performing meta-analysis of the PMBB and BioMe biobanks, we found that individuals with heterozygous LoF had increased incidence of end stage renal disease and dialysis ($P<0.05$) (table S1). Using extracted individual phenotype information we found that 36.1% of heterozygous LoF variants had CKD and 16.6% had ESRD, confirming our diagnosis code-based analysis (Fig.1C). Overall, our approach indicated that LoF coding variants in *MANBA* are associated with increased kidney disease incidence.

Manba knockout mice show increased severity of acute and chronic kidney disease

To understand the role of *Manba* in kidney disease development, we characterized genetically engineered *Manba* knock-out (*Manba*$^{-/-}$) mice. First we confirmed the decrease in *Manba* transcript expression, serum beta-mannosidase expression and beta-mannosidase enzyme activity in kidneys of *Manba*$^{-/-}$ mice. Heterozygous mice showed a 45% reduction in *Manba* transcripts in their kidneys. Serum beta-mannosidase and beta-mannosidase enzyme activity was reduced similarly (Fig. 2, A to C).

Gross phenotypic analysis of the *Manba* knock-out mice showed no obvious changes in body weight (fig. S9A), systolic blood pressure (fig. S9B), random blood glucose (fig. S9C), albuminuria (quantified as albumin/creatinine ratio) (fig. S9D), or kidney filtration parameters such as serum creatinine (fig. S9E), blood urea nitrogen (BUN) (fig. S9F) and *Lcn2 and Hacvr1* which encode NGAL and KIM-1, respectively (fig. S9G).

We next compared the injury response of control and *Manba* heterozygous and knock-out mice. First, we tested the renal response to folic acid injection. Folic acid precipitates in kidney tubules inducing acute injury initially, and later fibrosis. Kidneys of *Manba*$^{-/-}$ mice showed more severe tubular injury than control animals after folic acid injection. Structural changes analyzed on PAS-stained sections showed more severe tubule dilation, epithelial cell simplification, widened interstitium, and collagen and immune cell accumulation (Fig. 2D). Sirius red staining showed an increase in the accumulation of collagen in folic-acid injected *Manba*$^{-/-}$ mice, when compared to wild type folic acid injected animals (Fig. 2E). In line with the histological changes, QRT-PCR analysis indicated that transcript expressions of profibrotic genes including vimentin (*Vim*), fibronectin (*Fn*), procollagen1α1 (*Col1α1*), procol3α1 (*Col3α1)*, were markedly increased in *Manba*$^{-/-}$ mice compared to wild-type mice after folic acid injection (Fig. 2F). Immunoblots confirmed the increase in fibrotic markers, including α-SMA and fibronectin in *Manba*$^{-/-}$ mice compared to wild-type mice following folic acid injection (Fig. 2G).

Next we analyzed kidney disease severity in *Manba* heterozygous mice that mimic changes in *Manba* expression in subjects with the risk allele or heterozygous LoF. Cisplatin is a known nephrotoxic chemotherapeutic due to the uptake of platinum by the proximal tubules. Animals were injected 20 mg/kg cisplatin and wild-type, heterozygous and knock-out mice were sacrificed 3 days after the injection. Kidney structure analysis examined on H&E and Sirius red staining showed more severe tubule injury in *Manba*$^{+/-}$ and *Manba*$^{-/-}$ mice compared to wild-type animals (Fig. 3A and fig. S10, A and B). Wild-type mice developed modest injury as evident by serum BUN and creatinine, whereas *Manba* heterozygous and knock-out mice had higher BUN and creatinine following injury (Fig. 3B). Expression of kidney injury markers such as *Havcr1* and *Lcn2* were higher in cisplatin-injected *Manba*$^{+/-}$ and *Manba*$^{-/-}$ mice (Fig. 3C). Markers of chronic kidney disease and fibrosis such as *Vim*, transforming growth factor β1 (*Tgfβ1*), *Col1 α1*, and *Col3α1* were not changed in wild-type mice, but were markedly elevated in kidneys of cisplatin injected *Manba*$^{+/-}$ and *Manba*$^{-/-}$ mice (Fig. 3D). Protein expression of α-SMA and fibronectin, analyzed by Western blots, strongly correlated with transcript expressions (Fig. 3E). These studies indicate that *Manba*$^{-/-}$ and *Manba*$^{+/-}$ mice develop more severe kidney injury. In addition,

whereas wild-type mice showed minimal fibrotic changes, *Manba*$^{+/-}$ and *Manba*$^{-/-}$ mice developed evident renal fibrosis, indicating an AKI to CKD transition.

Manba deficiency reduces autophagic clearance in cultured kidney tubule cells

Analyzing mouse kidney single cell RNA sequencing datasets(18), we found that expression of *Manba* was the highest in kidney tubule cells such as the proximal tubules and collecting duct (Fig. 4A). Immunohistochemistry staining confirmed the expression of MANBA by tubule epithelial cells (Fig. 4B). *Cisd2* was not readily detectable (Fig. 4A), whereas *Nfkb1* and *Ube2d3* were expressed in fibroblasts and immune cells (Fig. 4A).

Next, we wanted to understand the molecular mechanism of *Manba* mediated protection from kidney damage. We isolated renal tubule cells from wild-type and *Manba*$^{-/-}$ mice and cultured them on filters so they remained polarized, which we confirmed by the tight junction marker zona occludens-1 (ZO-1) and microtubule marker end-binding protein-1 (EB-1) immunofluorescence stainings (fig. S11A).

Manba is a lysosomal gene and its deficiency causes lysosomal storage disease due to lysosomal dysfunction. To characterize lysosomal structure, we performed LAMP1 immunofluorescence staining. We found that lysosome number and size were increased in *Manba* knock-out tubule cells at baseline and after nutrient deprivation (Fig. 4C). Furthermore, lysosomes showed perinuclear distribution in *Manba* knockout tubule cells, compared to wild-type tubule cells, after starvation (Fig. 4C). LysoTracker staining further confirmed the increase in lysosomal number and size in *Manba* knock-out tubule cells (Fig. 4D).

Lysosomes play key roles in degrading cargo from endocytic vesicles and from autophagosomes. Therefore, we examined whether the structural defect observed in lysosomes also leads to functional changes in endocytosis and autophagy. We analyzed fluid-phase endocytosis using fluorescent labelled 10 kD dextran and found that dextran uptake was lower in *Manba* knock-out cells (Fig. 4E). Next, we examined receptor-mediated endocytosis using fluorescent labelled albumin and found that labelled albumin uptake was also lower in *Manba*$^{-/-}$ cells (Fig. 4F), indicating a defect in endocytosis.

To explore alterations in autophagic clearance, we examined autophagy flux in wild-type and *Manba*$^{-/-}$ cells. Cells were cultured in regular medium (fed) or nutrient poor (starved) conditions in the presence or absence of chloroquine (CQ) and bafilomycin A1(BafA1) to block lysosomal function and thereby lysosome-mediated degradation of autophagosomes. As expected, LC3BII, an autophagosomal marker, increased under nutrient deprivation. CQ and BafA1 further increased LC3BII as the lysosomal degradation of autophagosomes was blocked (Fig. 4, G and H), however, the change in LC3BII in *Manba*$^{-/-}$ cells was minimal. The difference was more pronounced at 4-hour compared to 2-hour time-point. LC3B immunofluorescence staining confirmed our findings (Fig. 4, I and J).

Defects in both autophagosome biogenesis and lysosomal fusion can lead to failure in LC3BII accumulation. During the assembly of the autophagosome, WIPI1 (WD repeat domain phosphoinositide-interacting protein 1) interacts with the lipid

phosphatidylinositol-3 phosphate (PI3P) and mediates the recruitment of the large multimeric complex of ATG12-ATG5-ATG16 (19). ULK1 (Unc-51 like autophagy activating kinase) is essential for autophagy and is activated by nutrient deprivation. ULK1 Ser757 phosphorylation is decreased by starvation, which disrupts the interaction between ULK1 and MAPK and activates autophagy (20). We analyzed these markers of autophagosome biogenesis and found that baseline P-ULK1 was higher in *Manba*$^{-/-}$ cells and the reduction of P-ULK1 (induced by starvation, CQ, or BafA1) was greater in wild-type cells, indicating a potential defect at the early stages of autophagy (fig. S11B). Immunoblotting analysis confirmed the immunostaining results (fig. S11C). WIPI1 increased in wild-type tubule epithelial cells (TECs) after a 4-hour nutrient deprivation, indicating an induction of autophagy, but changed minimally in *Manba*$^{-/-}$ TECs (fig. S11, D and E). Treatment with rapamycin a weak inducer of autophagy increased LC3BII but did not fully normalize autophagy flux in *Manba*$^{-/-}$ TECs (fig. S11F). In summary, by analyzing cultured TEC cells, we found that *Manba* deficient cells had marked structural lysosomal defects and showed alterations both in fluid phase and receptor mediated endocytosis and autophagy flux.

Mice with *Manba* loss show impaired autophagy

To determine whether our *in vitro* observations could be recapitulated *in vivo*, we analyzed *Manba* knock-out mice. In older *Manba*$^{-/-}$ mice, we observed visible accumulations of large vesicles in renal tubule cells by PAS staining (fig.S12A). Immunostaining with the lysosomal marker, LAMP1 indicated that these vesicles were lysosomes (Fig.5A). Lysosomal density was further increased in folic acid -treated mice (fig.S12B). Transmission electron microscopy analysis confirmed the increase in lysosome number (Fig.5B). Consistent with our *in vitro* studies, we also observed a defect in lysosomal structure such as lysosomal diameter was increased in *Manba*$^{-/-}$ mice (Fig. 5B).

We did not detect an observable change in LC3B at baseline, and found only minor changes in autophagy when comparing folic acid-treated and control kidney samples (Fig. 5C). On the other hand, LC3BII was markedly higher in folic acid-injected *Manba*$^{-/-}$ mice (Fig. 5C). Autophagic vacuole content analyzed by LC3B IF staining (fig. S12C) showed increased LC3 in folic acid-injected *Manba*$^{-/-}$ mice when compared to wild type FA injected animals. Sequestosome-1 (SQSTM1) is an autophagy cargo protein that targets other proteins for selective autophagy. Protein expression of SQSTM1 was increased in folic acid-injected *Manba*$^{-/-}$ mice (Fig. 5C), indicating a defect in autophagy.

Consistent with prior studies, we observed an increase in expression of LC3BII in the cisplatin induced model of kidney injury (21). The accumulation of LC3BII was greater in *Manba* heterozygous mice after cisplatin injection as compared to cisplatin-injected wild-type mice (Fig. 5D). Protein expression of SQSTM1 was higher in cisplatin-injected wild-type mice compared to control, and even higher in cisplatin-injected *Manba*$^{+/-}$ mice (Fig. 5D). Moreover, in cisplatin-injected *Manba*$^{-/-}$ mice, we observed enlarged lysosomes and increased LC3B accumulation compared to cisplatin-treated wild-type mice (Fig. 5, E and F). Western blot analysis indicated an increase in SQSTM1 expression in *Manba*$^{-/-}$ mice after injection of cisplatin (Fig. 5G). Taken together, our *in vivo* data indicated

an impairment of lysosomal functions and autophagy flux in *Manba* heterozygous and knockout mice, a finding consistent with our *in vitro* studies.

Loss of *Manba* leads to an increase in inflammatory cell death

Next, we aimed to understand the connection between an impaired auto-lysosomal function observed in *Manba* deficiency mice and kidney fibrosis development. Defects in lysosomes have been directly linked to inflammasome (NLRP3) activation and downstream pyroptosis (22). In addition, as autophagy plays a role in the clearance of injured cells, a defect in autophagy would result in an increase in other more inflammatory cell death pathways (for example pyroptosis).

We found minimal NLRP3 expression in folic acid-injected wild-type mice, however, NLRP3 expression was markedly increased in the folic acid-injected *Manba* knock-out mice (Fig. 6A). Expression of cleaved caspase1; the effector caspase in the pyroptosis pathway was also higher in folic acid-injected $Manba^{-/-}$ animals (Fig. 6A). Expression of inflammatory cytokines such as *Il-1β*, *Tnfα*, *Ccl2* mRNA were greater in folic acid-injected $Manba^{-/-}$ mice compared to folic acid-injected wild-type mice, consistent with the activation of an inflammatory cell death pathway (Fig. 6B).

Upon analyzing the cisplatin model of kidney injury, we found an increase in NLRP3 and caspase 1 expression in the cisplatin-injected $Manba^{-/-}$ mice, indicating inflammasome activation and pyroptosis (Fig. 6C). We also observed a marked increase in inflammatory and immune cell markers such as *Il-1β*, *Nlrp3*, *Tnfα*, *Ccl2*, *Cd68*, and *Lyz2* in cisplatin-injected $Manba^{-/-}$ mice (Fig. 6, D and E). To confirm that the increase in pyroptosis was related to kidney tubule cells, we analyzed wild-type, heterozygous, and knock-out cultured TECs. We found that the expression of *Nlrp3*, *Il-1β*, *Tnfα*, *Ccl2* was higher in $Manba^{-/-}$ TECs compared to wild-type TECs, indicating activation of the inflammasome in the cells (Fig. 6F). Taken together, these results suggest that loss of *Manba* leads to a defect in lysosomal structure and functions which directly or indirectly (via autophagy dysfunction) activates the inflammasome and shifts to a more inflammatory cell death mechanism (pyroptosis), resulting in a more severe inflammation and fibrosis in *Manba* heterozygous and knockout mice (Fig. 6G).

Deep-phenotyping of human kidney samples from CKD risk genotype subjects indicates a lysosomal defect and exacerbated inflammation

Last, we wanted to understand whether non-coding variants around *MANBA* were associated with observable changes in the endolysosomal system in patients with CKD. Immunostaining studies with the lysosomal marker LAMP1 indicated an increase in lysosome number and size in kidneys of subjects (n=3 in each group) with the risk allele compared to reference allele (Fig. 7A). Next, we analyzed gene expression changes in microdissected human kidney tubule samples from subjects (n=150) with risk or reference genotypes by RNA sequencing. We identified 50 genes that showed a nominally significant difference in kidneys of reference and risk allele subjects (table S2). Gene ontology analysis of differentially expressed genes indicated enrichment in immune system markers and immune system regulators in kidneys of patients with the risk allele (Fig. 7B). For example,

we found that the expression of *C1QL1* showed differences in subjects with risk and reference alleles, even after adjusting for important confounders such as age, race, and gender disease severity (Fig. 7C). In summary, analysis of kidneys from subjects with risk and reference alleles indicated a defect in lysosomal structure and immune cell activation, underlining the importance of these pathways in disease development in patients.

DISCUSSION

Here, we show that genetic variants on chromosome 4 that have been associated with kidney disease (such as $eGFR_{crea}$, BUN, and CKD) in multiple large genome-wide association studies also influence the expression of beta-mannosidase in human kidney tubule samples. Individuals with CKD risk variant had lower expression of *MANBA* in kidney tubules. Subjects who carried a rare heterozygous LoF *MANBA* variant also had an increased incidence of end stage kidney disease. Functional studies using mice with genetic loss of *Manba* indicated that kidney injury was more severe in mice with lower *Manba* expression. The defect seemed to be mediated by lysosomal dysfunction in $Manba^{-/-}$ mice, which lead to a block in endocytosis and autophagy, activation of the inflammasome, and an enhanced fibrotic response following a toxic injury.

We used an integrated approach for GWAS target identification that not only relied on multiple genotype-phenotype association studies but also examined multiple kidney eQTL datasets and data from more than 40 other organs. Our analysis clearly showed that variants associated with kidney function on chromosome 4 also modulate *MANBA* expression in human kidney tubule samples. This direction-specific association was replicated in glomeruli, whole kidney cortex samples, disease kidney tissue samples, and fibroblasts, indicating the robustness of this observation. At present, we cannot fully exclude that CKD GWAS genetic variants also associate with the expression of *CISD2*. The *CISD2* association was only observed in a single dataset, whereas the *MANBA* association was consistent in all datasets. Future studies can be aimed to understand the role of *CISD2* in the kidney.

Lysosomes are acidic intracellular compartments important for degradation of biomolecules. Extracellular proteins are taken up by endocytosis, whereas intracellular components are digested via autophagy (23). Genetic defects in lysosomal proteins result in lysosomal storage diseases. Kidney dysfunction is a major cause of morbidity and mortality in multiple lysosomal storage diseases, such as Fabry's disease and cystinosis (24). Fabry's disease is caused by deficiency of the enzyme alpha galactosidase A, leading to glycolipid globotriaosylceramide accumulation. *MANBA* encodes the beta-mannosidase that subcellularly localizes to the lysosome, where it is the final exoglycosidase for N-linked glycoprotein oligosaccharide catabolism (25). Patients with beta-mannosidosis have a wide spectrum of neurological involvement, including intellectual disability, hearing loss, ataxia, and seizures (26). Here, we recapitulated this phenotype spectrum even in subjects with heterozygous loss of function variants in our health system-based exome-sequencing cohorts. Beta mannosidase deletion is relatively common in ruminates (goats and calf) and associated with a more severe phenotype resulting in neonatal death (27, 28). The function of *MANBA* is still poorly understood, patients with *MANBA* mutations are diagnosed by increased urinary excretion of oligosaccharides. In 2006, the first *Manba* knock-out mice

displayed severe cytoplasmic vacuolization in the CNS and minimal vacuolation in most visceral organs along with tissue accumulation of non-degraded oligosaccharides and a compensatory upregulation of other lysosomal enzymes such as the alpha mannosidase and alkaline phosphatase(29). Future studies should analyze the renal phenotype of patients with homozygous *MANBA* mutations.

Our studies highlight the critical role of lysosomal integrity in protecting from kidney disease development. The renal glomerulus serves a size selective filter, where molecules smaller than around 60kD are filtered. This necessitates the uptake and recycling of a large number of biomolecules. Proximal tubule epithelial cells express high levels of the multiligand receptors such as megalin and cubilin, which mediate the efficient uptake of low molecular weight proteins and other ligands from the filtrate (30). The apical endocytic pathway in proximal tubule cells is uniquely specialized to accommodate the high capacity needs of these cells and is acutely and chronically regulated in response to changes in ligand exposure (31). Receptor-mediated endocytosis is strongly linked to lysosomal function. Mice that lack *Megalin* have low molecular weight proteinuria and lose lysosomal proteins in the urine, indicating a role for *Megalin* in recapturing these enzymes as well as in lysosomal biogenesis (32, 33).

Another key function of lysosomes is the direct digestion and degradation of endogenous proteins via autophagy(34). Genetic deletion of autophagy regulators such as *Atg5* and *Atg7* in kidney tubules indicated an important role for autophagy in tubule epithelial cell health and protection from injury (21, 35, 36). Autophagy flux relies on the degradative capacity of lysosomes, an impaired lysosomal function may explain the accumulation of autophagosomes in lysosomal storage diseases such as cystinosis (37). Although autophagy defect has been proposed to play a role in fibrosis development, its role is somewhat controversial (36, 38, 39). Defects in autophagy exacerbate most forms of acute kidney injury, which could lead to more severe fibrosis. Furthermore, autophagy is also a key mechanism for retrieval of stored lipids for oxidation (34) and eliminating dysfunctional mitochondria by mitophagy. Kidney tubule cells strongly rely on fatty acid oxidation and oxidative phosphorylation as their major energy source, a defect in autophagy could easily disturb energy homeostasis as well (40). Here we show that the *MANBA*-induced lysosomal dysfunction and defect in autophagy resulted in inflammasome (NLRP3) activation, pyroptosis, and inflammatory cell death. This is likely to be the key mechanism of *MANBA* deficiency-induced kidney disease development, and this effect seems to be more pronounced during aging or a toxic injury. Whereas a toxic injury (cisplatin) is associated with an acute injury and recovery in wild-type mice, we observed a profibrotic response in the *Manba* knock-out mice.

A key strength of the study is the systematic common and rare variant analysis, the identification of a new disease-causing gene and mechanism. Our results indicate that GWAS and eQTL data are powerful for causal gene identification, and analyzing subjects with heterozygous LoF could provide important avenues to understand phenotype development. The phenotypes in subjects with *MANBA* LoF were neuropsychiatric and pulmonary diseases. End-stage kidney disease and renal dialysis reached nominal significance in the meta-analysis. Future larger studies using this approach might be able

to refine the phenotype with better precision, as full PheWAS studies are heavily penalized for the multiple comparisons.

Our study has several limitations; such as we used kidney function-based GWAS studies not variants *per se* associated with CKD. Future studies shall analyze the role of *CISD2* in kidney disease development, in addition, the role of inflammasome activation in *MANBA*-associated kidney disease development should be formally tested using genetically modified animal models. Our finding could open new avenues for therapeutic targeting of the autolysosomal pathways in kidney disease development.

In conclusion, here we identified *MANBA* as a kidney disease severity gene through the integration of the CKD GWAS, eQTL,and exome analysis. We show that deletion of *Manba* exacerbated kidney injury in animal models mostly via lysosomal derangement.

MATERIALS AND METHODS

Study design

The objective of this study was to understand the role of *MANBA* in kidney disease development. Computational integration of common genetic variants (from GWAS) associated with kidney function and human kidney eQTL studies prioritized *MANBA* as a likely causal gene. We analyzed the phenotypes (PheWAS) of subjects with rare heterozygous loss of function variants in *MANBA* and studied kidney disease development in mice with genetic deletion of *MANBA*. For in vivo studies, we used littermates. Animals (wild type, heterozygous, or knock-out) from the same litter were randomly assigned to sham, folic acid, or cisplatin injection. The number of replicates (n>3) is indicated in the figure legends. Sample processing was performed simultaneously and in parallel for all conditions within each experiment. Renal sections were scored by an independent pathologist (M.P.) who was not aware of the disease state or genotype.

Study populations

Participants in the Penn Medicine Biobank were recruited from throughout the clinical practice sites of the University of Pennsylvania Health System. Participants were consented for bio-specimen storage, access to electronic health record data, and permission to recontact. Whole exome sequences were generated from DNA extracted from stored buffy coats by the Regeneron Genetics Center and mapped to Genome Reference Consortium Build 38 (GRCh38) as described elsewhere.

The BioMe Biobank is an EHR-linked clinical care cohort comprised of participants from diverse ancestries (African, Hispanic/Latino, European and Other ancestries). Participants in this analysis were recruited between 2007 and 2015. Enrollment of participants was predominantly through ambulatory care practices. Genetic data was linked to a wide array of longitudinal biomedical traits including clinical outcomes, imaging results, exposure data, originating from Mount Sinai's system-wide Epic EHR. The study was approved by each institution's Institutional Review Board.

Animal studies

Animal care and experiments were performed in accordance with the National Institutes of Health guidelines and approved by the Animal Care Committee at Perelman School of Medicine, University of Pennsylvania. *Manba* heterozygous mice was a kind gift of Professor Karen H. Friderici from Michigan State University (29). For the folic acid injury model, mice 8–10 weeks of age were intraperitoneally injected with folic acid (250 mg/kg, dissolved in 300 mM NaHCO3) and sacrificed 7 days after injection. For the cisplatin injury model. mice 6–8 weeks of age were intraperitoneally injected with cisplatin (20mg/kg, Cayman Chemical) in saline and sacrificed 3 days after injection.

Primary culture of mouse TECs

Kidneys were collected from 3–6 week-sold mice, minced and digested by 2 mg/ml collagenase I for 30 mins at 37 °C and then filtered successively through 100 μm, 70 μm and 40 μm mesh to collect single TEC cells. Cells were cultured in RPMI 1640 supplement with 10% FBS, 20 ng/ml EGF, and 100X ITS at 5% CO_2, 37 °C. At 80% confluence, cells were treated in fed condition (RPMI+10%FBS), or starved in HBSS with or without 50μM Chloroquine (CQ) or 50nM Bafilomycin A1(BafA1) for 2 or 4 hours.

Statistical analyses

Statistical tests were chosen based on nature of the variable (continuous or discrete) and data distribution (normal or skewed). The continuous variables with normal distribution were presented as mean ± S.E.M; non-normal variables were presented as median(interquartile range). Unpaired Student's t-test was used for comparisons between two groups. When needed multiple testing correction was performed by one-way or Two-way ANOVA with Tukey's post hoc tests. Data sets for which we could not determine normality were assessed using nonparametric statistical tests such as Mann-Whitney for comparisons between two groups or Kruskal-Wallis test for comparisons among more than two groups followed by Conover-Iman test with Bonferroni adjustment for multiple comparisons. P value < 0.05 was considered to be significant.

Supplementary Material

Refer to Web version on PubMed Central for supplementary material.

Acknowledgement:

We thank the staff of the Regeneron Genetics Center for whole-exome sequencing of DNA from PMBB participants. The Penn Medicine Biobank is supported by the Perelman School of Medicine at the University of Pennsylvania, a gift from the Smilow family, and the National Center for Advancing Translational Sciences of the National Institutes of Health under CTSA Award Number UL1TR001878.

Funding:

This work was supported by the NIH grants R01DK076077, R01DK087635, R01DK105821, and DP3 DK108220 (to K.S.); Shanghai Pujiang Program 18PJD049 (to X.G.); MVP BX003360 (to A.H.); NCATS UL1TR001878 (to D.R.); US Department of Veterans Affairs award IK2-CX001780 (to S.M.D.). This publication does not represent the views of the Department of Veterans Affairs or the United States government.

Competing interests:

Scott Damrauer received research support from RenalytixAI and consulting fees from Calico Labs outside of the current work. Girish Nadkarni: RenalytixAI (SAB member, Co-founder, own equity); Pensieve Health (SAB member, Co-founder, own equity. Girish Nadkarni is a paid consultant at Renalytix AI, Astra Zeneca, Reata, BioVie. Dr Susztak in member of the SAB of Jnana and consulted for Astra Zeneca, GSK, Jansen, Jnana Maze and Calico Labs. Research in the Susztak lab is also supported by GSK, Boehringer Ingelheim, Novo Nordisk, Regeneron, Gilead Merck and Bayer. The other authors declare that they have no competing interests.

Data and materials availability:

All data associated with this study are present in the paper or Supplementary Materials. Primary data are in data file S1.

REFERENCES AND NOTES

1. Eckardt KU, Coresh J, Devuyst O, Johnson RJ, Kottgen A, Levey AS, Levin A, Evolving importance of kidney disease: from subspecialty to global health burden. Lancet (London, England) 382, 158–169 (2013).
2. Raggi P, Su S, Karohl C, Veledar E, Rojas-Campos E, Vaccarino V, Heritability of renal function and inflammatory markers in adult male twins. Am J Nephrol 32, 317–323 (2010). [PubMed: 20720405]
3. Stranger BE, Stahl EA, Raj T, Progress and promise of genome-wide association studies for human complex trait genetics. Genetics 187, 367–383 (2011). [PubMed: 21115973]
4. Pattaro C, Teumer A, Gorski M, Chu AY, Li M, Mijatovic V, Garnaas M, Tin A, Sorice R, Li Y, Taliun D, Olden M, Foster M, Yang Q, Chen MH, Pers TH, Johnson AD, Ko YA, Fuchsberger C, Tayo B, Nalls M, Feitosa MF, Isaacs A, Dehghan A, d'Adamo P, Adeyemo A, Dieffenbach AK, Zonderman AB, Nolte IM, van der Most PJ, Wright AF, Shuldiner AR, Morrison AC, Hofman A, Smith AV, Dreisbach AW, Franke A, Uitterlinden AG, Metspalu A, Tonjes A, Lupo A, Robino A, Johansson A, Demirkan A, Kollerits B, Freedman BI, Ponte B, Oostra BA, Paulweber B, Kramer BK, Mitchell BD, Buckley BM, Peralta CA, Hayward C, Helmer C, Rotimi CN, Shaffer CM, Muller C, Sala C, van Duijn CM, Saint-Pierre A, Ackermann D, Shriner D, Ruggiero D, Toniolo D, Lu Y, Cusi D, Czamara D, Ellinghaus D, Siscovick DS, Ruderfer D, Gieger C, Grallert H, Rochtchina E, Atkinson EJ, Holliday EG, Boerwinkle E, Salvi E, Bottinger EP, Murgia F, Rivadeneira F, Ernst F, Kronenberg F, Hu FB, Navis GJ, Curhan GC, Ehret GB, Homuth G, Coassin S, Thun GA, Pistis G, Gambaro G, Malerba G, Montgomery GW, Eiriksdottir G, Jacobs G, Li G, Wichmann HE, Campbell H, Schmidt H, Wallaschofski H, Volzke H, Brenner H, Kroemer HK, Kramer H, Lin H, Leach IM, Ford I, Guessous I, Rudan I, Prokopenko I, Borecki I, Heid IM, Kolcic I, Persico I, Jukema JW, Wilson JF, Felix JF, Divers J, Lambert JC, Stafford JM, Gaspoz JM, Smith JA, Faul JD, Wang JJ, Ding J, Hirschhorn JN, Attia J, Whitfield JB, Chalmers J, Viikari J, Coresh J, Denny JC, Karjalainen J, Fernandes JK, Endlich K, Butterbach K, Keene KL, Lohman K, Portas L, Launer LJ, Lyytikainen LP, Yengo L, Franke L, Ferrucci L, Rose LM, Kedenko L, Rao M, Struchalin M, Kleber ME, Cavalieri M, Haun M, Cornelis MC, Ciullo M, Pirastu M, de Andrade M, McEvoy MA, Woodward M, Adam M, Cocca M, Nauck M, Imboden M, Waldenberger M, Pruijm M, Metzger M, Stumvoll M, Evans MK, Sale MM, Kahonen M, Boban M, Bochud M, Rheinberger M, Verweij N, Bouatia-Naji N, Martin NG, Hastie N, Probst-Hensch N, Soranzo N, Devuyst O, Raitakari O, Gottesman O, Franco OH, Polasek O, Gasparini P, Munroe PB, Ridker PM, Mitchell P, Muntner P, Meisinger C, Smit JH, I. Consortium, A. Consortium, Cardiogram, C. H.-H. F. Group, E. C. Consortium, Kovacs P, Wild PS, Froguel P, Rettig R, Magi R, Biffar R, Schmidt R, Middelberg RP, Carroll RJ, Penninx BW, Scott RJ, Katz R, Sedaghat S, Wild SH, Kardia SL, Ulivi S, Hwang SJ, Enroth S, Kloiber S, Trompet S, Stengel B, Hancock SJ, Turner ST, Rosas SE, Stracke S, Harris TB, Zeller T, Zemunik T, Lehtimaki T, Illig T, Aspelund T, Nikopensius T, Esko T, Tanaka T, Gyllensten U, Volker U, Emilsson V, Vitart V, Aalto V, Gudnason V, Chouraki V, Chen WM, Igl W, Marz W, Koenig W, Lieb W, Loos RJ, Liu Y, Snieder H, Pramstaller PP, Parsa A, O'Connell JR, Susztak K, Hamet P, Tremblay J, de Boer IH, Boger CA, Goessling W, Chasman DI, Kottgen A, Kao WH, Fox CS, Genetic associations at 53 loci highlight cell types and biological pathways relevant for kidney function. Nat Commun 7, 10023 (2016). [PubMed: 26831199]

5. Ko YA, Yi H, Qiu C, Huang S, Park J, Ledo N, Kottgen A, Li H, Rader DJ, Pack MA, Brown CD, Susztak K, Genetic-Variation-Driven Gene-Expression Changes Highlight Genes with Important Functions for Kidney Disease. Am J Hum Genet 100, 940–953 (2017). [PubMed: 28575649]

6. Lappalainen T, Scott AJ, Brandt M, Hall IM, Genomic Analysis in the Age of Human Genome Sequencing. Cell 177, 70–84 (2019). [PubMed: 30901550]

7. Sullivan KM, Susztak K, Unravelling the complex genetics of common kidney diseases: from variants to mechanisms. Nat Rev Nephrol, (2020).

8. Qiu C, Huang S, Park J, Park Y, Ko YA, Seasock MJ, Bryer JS, Xu XX, Song WC, Palmer M, Hill J, Guarnieri P, Hawkins J, Boustany-Kari CM, Pullen SS, Brown CD, Susztak K, Renal compartment-specific genetic variation analyses identify new pathways in chronic kidney disease. Nature medicine 24, 1721–1731 (2018).

9. G. T. Consortium, Human genomics. The Genotype-Tissue Expression (GTEx) pilot analysis: multitissue gene regulation in humans. Science 348, 648–660 (2015). [PubMed: 25954001]

10. Gillies CE, Putler R, Menon R, Otto E, Yasutake K, Nair V, Hoover P, Lieb D, Li S, Eddy S, Fermin D, McNulty MT, Nephrotic Syndrome Study N, Hacohen N, Kiryluk K, Kretzler M, Wen X, Sampson MG, An eQTL Landscape of Kidney Tissue in Human Nephrotic Syndrome. Am J Hum Genet 103, 232–244 (2018). [PubMed: 30057032]

11. Trudu M, Janas S, Lanzani C, Debaix H, Schaeffer C, Ikehata M, Citterio L, Demaretz S, Trevisani F, Ristagno G, Glaudemans B, Laghmani K, Dell'Antonio G, team S, Loffing J, Rastaldi MP, Manunta P, Devuyst O, Rampoldi L, Common noncoding UMOD gene variants induce salt-sensitive hypertension and kidney damage by increasing uromodulin expression. Nat Med 19, 1655–1660 (2013). [PubMed: 24185693]

12. Hellwege JN, Velez Edwards DR, Giri A, Qiu C, Park J, Torstenson ES, Keaton JM, Wilson OD, Robinson-Cohen C, Chung CP, Roumie CL, Klarin D, Damrauer SM, DuVall SL, Siew E, Akwo EA, Wuttke M, Gorski M, Li M, Li Y, Gaziano JM, Wilson PWF, Tsao PS, O'Donnell CJ, Kovesdy CP, Pattaro C, Kottgen A, Susztak K, Edwards TL, Hung AM, Mapping eGFR loci to the renal transcriptome and phenome in the VA Million Veteran Program. Nat Commun 10, 3842 (2019). [PubMed: 31451708]

13. Graham SE, Nielsen JB, Zawistowski M, Zhou W, Fritsche LG, Gabrielsen ME, Skogholt AH, Surakka I, Hornsby WE, Fermin D, Larach DB, Kheterpal S, Brummett CM, Lee S, Kang HM, Abecasis GR, Romundstad S, Hallan S, Sampson MG, Hveem K, Willer CJ, Sex-specific and pleiotropic effects underlying kidney function identified from GWAS meta-analysis. Nat Commun 10, 1847 (2019). [PubMed: 31015462]

14. Morris AP, Le TH, Wu H, Akbarov A, van der Most PJ, Hemani G, Smith GD, Mahajan A, Gaulton KJ, Nadkarni GN, Valladares-Salgado A, Wacher-Rodarte N, Mychaleckyj JC, Dueker ND, Guo X, Hai Y, Haessler J, Kamatani Y, Stilp AM, Zhu G, Cook JP, Arnlov J, Blanton SH, de Borst MH, Bottinger EP, Buchanan TA, Cechova S, Charchar FJ, Chu PL, Damman J, Eales J, Gharavi AG, Giedraitis V, Heath AC, Ipp E, Kiryluk K, Kramer HJ, Kubo M, Larsson A, Lindgren CM, Lu Y, Madden PAF, Montgomery GW, Papanicolaou GJ, Raffel LJ, Sacco RL, Sanchez E, Stark H, Sundstrom J, Taylor KD, Xiang AH, Zivkovic A, Lind L, Ingelsson E, Martin NG, Whitfield JB, Cai J, Laurie CC, Okada Y, Matsuda K, Kooperberg C, Chen YI, Rundek T, Rich SS, Loos RJF, Parra EJ, Cruz M, Rotter JI, Snieder H, Tomaszewski M, Humphreys BD, Franceschini N, Trans-ethnic kidney function association study reveals putative causal genes and effects on kidney-specific disease aetiologies. Nat Commun 10, 29 (2019). [PubMed: 30604766]

15. Wuttke M, Li Y, Li M, Sieber KB, Feitosa MF, Gorski M, Tin A, Wang L, Chu AY, Hoppmann A, Kirsten H, Giri A, Chai JF, Sveinbjornsson G, Tayo BO, Nutile T, Fuchsberger C, Marten J, Cocca M, Ghasemi S, Xu Y, Horn K, Noce D, van der Most PJ, Sedaghat S, Yu Z, Akiyama M, Afaq S, Ahluwalia TS, Almgren P, Amin N, Arnlov J, Bakker SJL, Bansal N, Baptista D, Bergmann S, Biggs ML, Biino G, Boehnke M, Boerwinkle E, Boissel M, Bottinger EP, Boutin TS, Brenner H, Brumat M, Burkhardt R, Butterworth AS, Campana E, Campbell A, Campbell H, Canouil M, Carroll RJ, Catamo E, Chambers JC, Chee ML, Chee ML, Chen X, Cheng CY, Cheng Y, Christensen K, Cifkova R, Ciullo M, Concas MP, Cook JP, Coresh J, Corre T, Sala CF, Cusi D, Danesh J, Daw EW, de Borst MH, De Grandi A, de Mutsert R, de Vries APJ, Degenhardt F, Delgado G, Demirkan A, Di Angelantonio E, Dittrich K, Divers J, Dorajoo R, Eckardt KU, Ehret G, Elliott P, Endlich K, Evans MK, Felix JF, Foo VHX, Franco OH, Franke A, Freedman BI, Freitag-Wolf S, Friedlander Y, Froguel P, Gansevoort RT, Gao H, Gasparini P,

Gaziano JM, Giedraitis V, Gieger C, Girotto G, Giulianini F, Gogele M, Gordon SD, Gudbjartsson DF, Gudnason V, Haller T, Hamet P, Harris TB, Hartman CA, Hayward C, Hellwege JN, Heng CK, Hicks AA, Hofer E, Huang W, Hutri-Kahonen N, Hwang SJ, Ikram MA, Indridason OS, Ingelsson E, Ising M, Jaddoe VWV, Jakobsdottir J, Jonas JB, Joshi PK, Josyula NS, Jung B, Kahonen M, Kamatani Y, Kammerer CM, Kanai M, Kastarinen M, Kerr SM, Khor CC, Kiess W, Kleber ME, Koenig W, Kooner JS, Korner A, Kovacs P, Kraja AT, Krajcoviechova A, Kramer H, Kramer BK, Kronenberg F, Kubo M, Kuhnel B, Kuokkanen M, Kuusisto J, La Bianca M, Laakso M, Lange LA, Langefeld CD, Lee JJ, Lehne B, Lehtimaki T, Lieb W, Lifelines Cohort S, Lim SC, Lind L, Lindgren CM, Liu J, Liu J, Loeffler M, Loos RJF, Lucae S, Lukas MA, Lyytikainen LP, Magi R, Magnusson PKE, Mahajan A, Martin NG, Martins J, Marz W, Mascalzoni D, Matsuda K, Meisinger C, Meitinger T, Melander O, Metspalu A, Mikaelsdottir EK, Milaneschi Y, Miliku K, Mishra PP, Program VAMV, Mohlke KL, Mononen N, Montgomery GW, Mook-Kanamori DO, Mychaleckyj JC, Nadkarni GN, Nalls MA, Nauck M, Nikus K, Ning B, Nolte IM, Noordam R, O'Connell J, O'Donoghue ML, Olafsson I, Oldehinkel AJ, Orho-Melander M, Ouwehand WH, Padmanabhan S, Palmer ND, Palsson R, Penninx B, Perls T, Perola M, Pirastu M, Pirastu N, Pistis G, Podgornaia AI, Polasek O, Ponte B, Porteous DJ, Poulain T, Pramstaller PP, Preuss MH, Prins BP, Province MA, Rabelink TJ, Raffield LM, Raitakari OT, Reilly DF, Rettig R, Rheinberger M, Rice KM, Ridker PM, Rivadeneira F, Rizzi F, Roberts DJ, Robino A, Rossing P, Rudan I, Rueedi R, Ruggiero D, Ryan KA, Saba Y, Sabanayagam C, Salomaa V, Salvi E, Saum KU, Schmidt H, Schmidt R, Schottker B, Schulz CA, Schupf N, Shaffer CM, Shi Y, Smith AV, Smith BH, Soranzo N, Spracklen CN, Strauch K, Stringham HM, Stumvoll M, Svensson PO, Szymczak S, Tai ES, Tajuddin SM, Tan NYQ, Taylor KD, Teren A, Tham YC, Thiery J, Thio CHL, Thomsen H, Thorleifsson G, Toniolo D, Tonjes A, Tremblay J, Tzoulaki I, Uitterlinden AG, Vaccargiu S, van Dam RM, van der Harst P, van Duijn CM, Velez Edward DR, Verweij N, Vogelezang S, Volker U, Vollenweider P, Waeber G, Waldenberger M, Wallentin L, Wang YX, Wang C, Waterworth DM, Bin Wei W, White H, Whitfield JB, Wild SH, Wilson JF, Wojczynski MK, Wong C, Wong TY, Xu L, Yang Q, Yasuda M, Yerges-Armstrong LM, Zhang W, Zonderman AB, Rotter JI, Bochud M, Psaty BM, Vitart V, Wilson JG, Dehghan A, Parsa A, Chasman DI, Ho K, Morris AP, Devuyst O, Akilesh S, Pendergrass SA, Sim X, Boger CA, Okada Y, Edwards TL, Snieder H, Stefansson K, Hung AM, Heid IM, Scholz M, Teumer A, Kottgen A, Pattaro C, A catalog of genetic loci associated with kidney function from analyses of a million individuals. Nat Genet 51, 957–972 (2019). [PubMed: 31152163]

16. Giambartolomei C, Vukcevic D, Schadt EE, Franke L, Hingorani AD, Wallace C, Plagnol V, Bayesian test for colocalisation between pairs of genetic association studies using summary statistics. PLoS Genet 10, e1004383 (2014). [PubMed: 24830394]
17. Bedilu R, Nummy KA, Cooper A, Wevers R, Smeitink J, Kleijer WJ, Friderici KH, Variable clinical presentation of lysosomal beta-mannosidosis in patients with null mutations. Mol Genet Metab 77, 282–290 (2002). [PubMed: 12468273]
18. Park J, Shrestha R, Qiu C, Kondo A, Huang S, Werth M, Li M, Barasch J, Susztak K, Single-cell transcriptomics of the mouse kidney reveals potential cellular targets of kidney disease. Science 360, 758–763 (2018). [PubMed: 29622724]
19. Grimmel M, Backhaus C, Proikas-Cezanne T, WIPI-Mediated Autophagy and Longevity. Cells 4, 202–217 (2015). [PubMed: 26010754]
20. Nwadike C, Williamson LE, Gallagher LE, Guan JL, Chan EYW, AMPK Inhibits ULK1-Dependent Autophagosome Formation and Lysosomal Acidification via Distinct Mechanisms. Mol Cell Biol 38, (2018).
21. Jiang M, Wei Q, Dong G, Komatsu M, Su Y, Dong Z, Autophagy in proximal tubules protects against acute kidney injury. Kidney Int 82, 1271–1283 (2012). [PubMed: 22854643]
22. Swanson KV, Deng M, Ting JP, The NLRP3 inflammasome: molecular activation and regulation to therapeutics. Nat Rev Immunol 19, 477–489 (2019). [PubMed: 31036962]
23. Platt FM, Boland B, van der Spoel AC, The cell biology of disease: lysosomal storage disorders: the cellular impact of lysosomal dysfunction. J Cell Biol 199, 723–734 (2012). [PubMed: 23185029]
24. Surendran K, Vitiello SP, Pearce DA, Lysosome dysfunction in the pathogenesis of kidney diseases. Pediatr Nephrol 29, 2253–2261 (2014). [PubMed: 24217784]

25. Gytz H, Liang J, Liang Y, Gorelik A, Illes K, Nagar B, The structure of mammalian beta-mannosidase provides insight into beta-mannosidosis and nystagmus. FEBS J 286, 1319–1331 (2019). [PubMed: 30552791]
26. Huynh T, Khan JM, Ranganathan S, A comparative structural bioinformatics analysis of inherited mutations in beta-D-Mannosidase across multiple species reveals a genotype-phenotype correlation. BMC genomics 12 Suppl 3, S22 (2011). [PubMed: 22369051]
27. Jones MZ, Cunningham JG, Dade AW, Alessi DM, Mostosky UV, Vorro JR, Benitez JT, Lovell KL, Caprine beta-mannosidosis: clinical and pathological features. J Neuropathol Exp Neurol 42, 268–285 (1983). [PubMed: 6842266]
28. Abbitt B, Jones MZ, Kasari TR, Storts RW, Templeton JW, Holland PS, Castenson PE, Beta-mannosidosis in twelve Salers calves. J Am Vet Med Assoc 198, 109–113 (1991). [PubMed: 1995562]
29. Zhu M, Lovell KL, Patterson JS, Saunders TL, Hughes ED, Friderici KH, Beta-mannosidosis mice: a model for the human lysosomal storage disease. Hum Mol Genet 15, 493–500 (2006). [PubMed: 16377659]
30. Nielsen R, Christensen EI, Birn H, Megalin and cubilin in proximal tubule protein reabsorption: from experimental models to human disease. Kidney Int 89, 58–67 (2016). [PubMed: 26759048]
31. Eshbach ML, Weisz OA, Receptor-Mediated Endocytosis in the Proximal Tubule. Annu Rev Physiol 79, 425–448 (2017). [PubMed: 27813828]
32. Christensen EI, Moskaug JO, Vorum H, Jacobsen C, Gundersen TE, Nykjaer A, Blomhoff R, Willnow TE, Moestrup SK, Evidence for an essential role of megalin in transepithelial transport of retinol. J Am Soc Nephrol 10, 685–695 (1999). [PubMed: 10203351]
33. Birn H, Willnow TE, Nielsen R, Norden AG, Bonsch C, Moestrup SK, Nexo E, Christensen EI, Megalin is essential for renal proximal tubule reabsorption and accumulation of transcobalamin-B(12). Am J Physiol Renal Physiol 282, F408–416 (2002). [PubMed: 11832420]
34. Ryter SW, Bhatia D, Choi ME, Autophagy: A Lysosome-Dependent Process with Implications in Cellular Redox Homeostasis and Human Disease. Antioxid Redox Signal 30, 138–159 (2019). [PubMed: 29463101]
35. Gu X, Raman A, Susztak K, Going from acute to chronic kidney injury with FoxO3. J Clin Invest 130, 2192–2194 (2019).
36. Li L, Kang H, Zhang Q, D'Agati VD, Al-Awqati Q, Lin F, FoxO3 activation in hypoxic tubules prevents chronic kidney disease. J Clin Invest 129, 2374–2389 (2019). [PubMed: 30912765]
37. Festa BP, Chen Z, Berquez M, Debaix H, Tokonami N, Prange JA, Hoek GV, Alessio C, Raimondi A, Nevo N, Giles RH, Devuyst O, Luciani A, Impaired autophagy bridges lysosomal storage disease and epithelial dysfunction in the kidney. Nat Commun 9, 161 (2018). [PubMed: 29323117]
38. Ding Y, Kim S, Lee SY, Koo JK, Wang Z, Choi ME, Autophagy regulates TGF-beta expression and suppresses kidney fibrosis induced by unilateral ureteral obstruction. J Am Soc Nephrol 25, 2835–2846 (2014). [PubMed: 24854279]
39. Livingston MJ, Ding HF, Huang S, Hill JA, Yin XM, Dong Z, Persistent activation of autophagy in kidney tubular cells promotes renal interstitial fibrosis during unilateral ureteral obstruction. Autophagy 12, 976–998 (2016). [PubMed: 27123926]
40. Kang HM, Ahn SH, Choi P, Ko YA, Han SH, Chinga F, Park AS, Tao J, Sharma K, Pullman J, Bottinger EP, Goldberg IJ, Susztak K, Defective fatty acid oxidation in renal tubular epithelial cells has a key role in kidney fibrosis development. Nat Med 21, 37–46 (2015). [PubMed: 25419705]

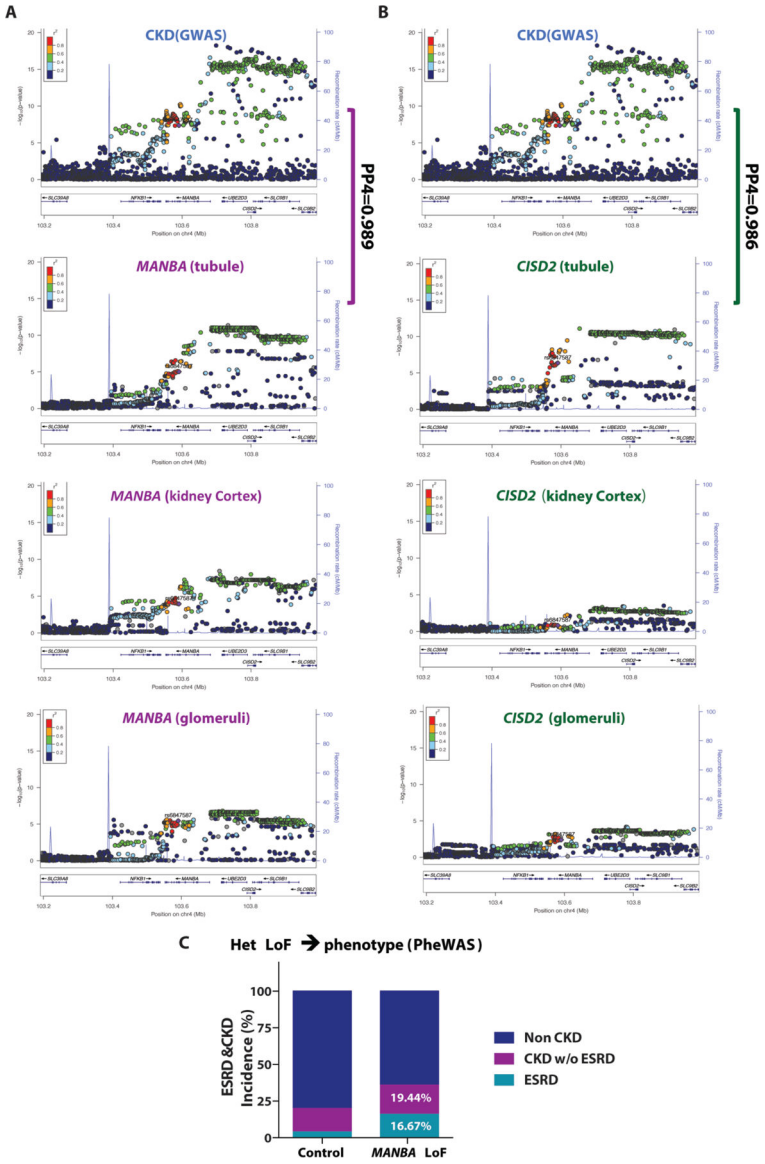

Fig. 1. Common (GWAS) and rare variant (PheWAS) analysis identifies an association between *MANBA*, kidney function, and kidney disease.

(A and B) LocusZoom plots of chromosome 4 region of CKD eGFR GWAS(15), *MANBA* eQTL and *CISD2* eQTL in whole kidneys(5), glomeruli, and tubules(8). X-axis shows the chromosomal location of SNPs. Y-axis shows the strength of association or recombination rate. **(C)** Distribution of non-CKD, CKD without ESRD, and ESRD subjects amongst the identified *MANBA* heterozygous LOF alleles compared to subjects in the Biome and PMBB biobanks. Y-axis shows the percentage of the disease distributions.

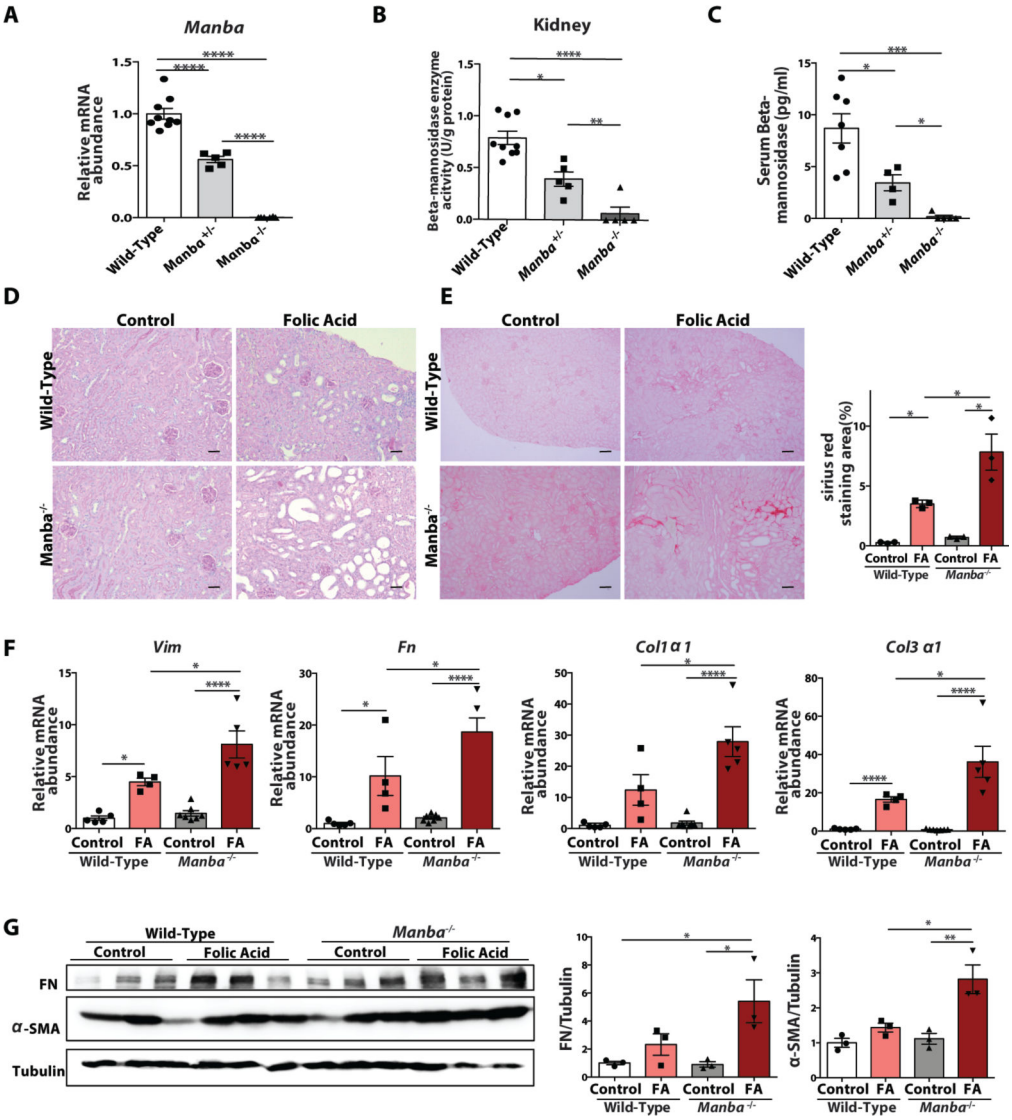

Fig. 2. *Manba* deficiency exacerbates fibrosis in a folic acid-induced kidney injury model

(A) *Manba* expression of wild-type, $Manba^{+/-}$, and $Manba^{-/-}$ mice determined by real-time PCR (n= 5 to 9 animals per group). **(B)** Beta-Mannosidase activity was assayed in kidney tissues of wild-type, $Manba^{+/-}$, and $Manba^{-/-}$ mice (n=5 to 9 animals per group). **(C)** Serum beta-Mannosidase expression in wild-type mice, $Manba^{+/-}$, and $Manba^{-/-}$ mice (n=5 to 7 animals per group). **(D)** Representative images of PAS-stained kidney sections from wild-type and $Manba^{-/-}$ mice 7 days after sham or folic acid (FA) injection. Scale bar, 20μm. **(E)** Representative images of Sirius Red-stained kidney sections from wild-type and $Manba^{-/-}$ mice 7 days after sham or FA injection. Scale bar, 50μm. Quantification of Sirius Red-staining (n=3 per group). **(F)** Relative mRNA abundance of *Vim, Fn, Colα1*, and *Col3α1*, in wild-type and $Manba^{-/-}$ mice kidneys 7 days after sham or FA injection (n=4 to 7 animals per group). **(G)** Representative Western blots of fibronectin andα-SMA of kidney tissues of wild-type and $Manba^{-/-}$ mice 7 days after sham or FA injection (n = 3 per group). Densitometry analysis was performed to quantify protein expression. Data shown are

means ± SEM. Statistical analysis by **(A to C, and F to G)** One-way ANOVA with Tukey's post-hoc test, *$P < 0.05$, **$P < 0.01$, ***$P < 0.001$, **** $P < 0.0001$.

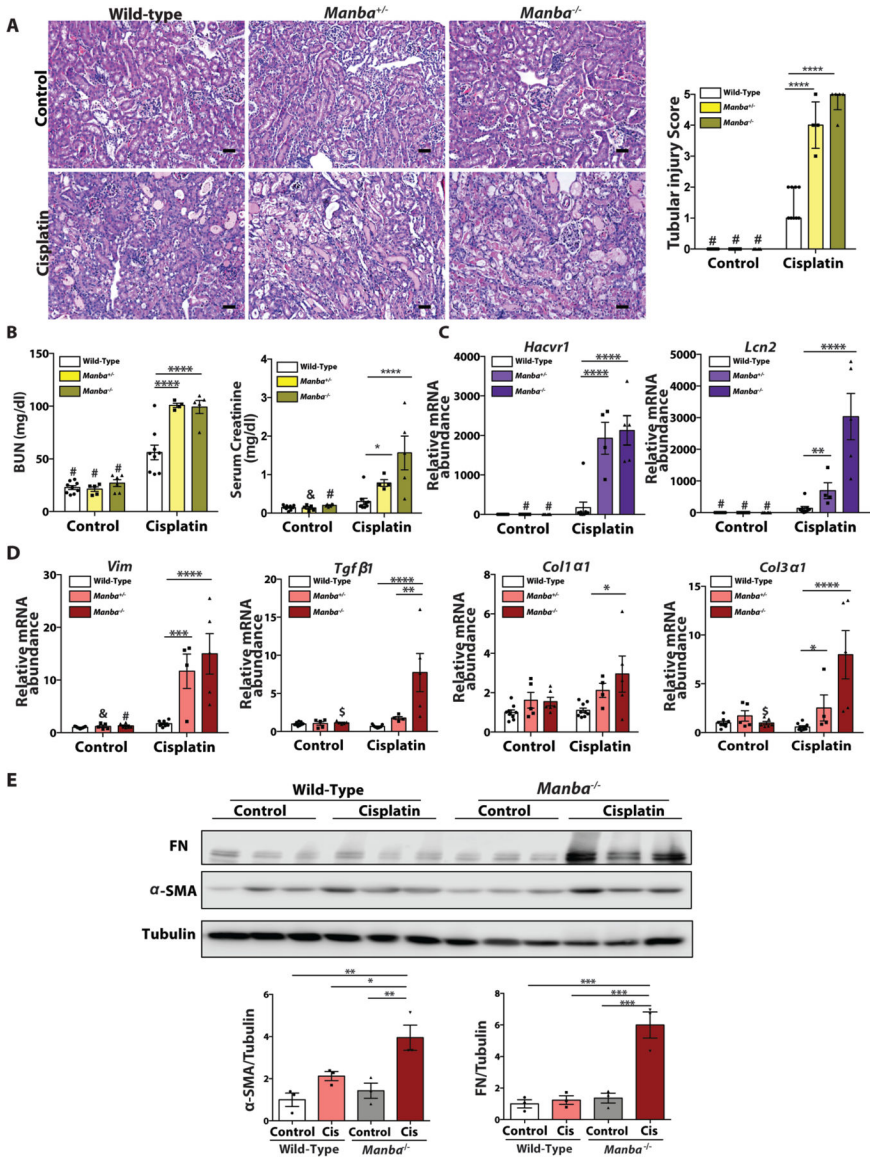

Fig. 3. Genetic deletion of *Manba* exacerbates cisplatin-induced kidney injury.

(A) Representative images of H&E-stained kidney sections from wild-type, *Manba*$^{+/-}$ and *Manba*$^{-/-}$ mice 3 days after sham or cisplatin injection. Scale bar, 20μm. Tubular injury scores of kidney sections of wild-type, *Manba*$^{+/-}$, and *Manba*$^{-/-}$ mice 3 days after sham or cisplatin injection. **(B)** BUN and serum creatinine of wild-type, *Manba*$^{+/-}$, and *Manba*$^{-/-}$ mice 3 days after sham or cisplatin injection. **(C and D)** Relative mRNA abundance of *Lcn2, Hacvr1, Vim, Tgfβ1, Colα1*, and *Col3α1* in kidneys of wild-type, *Manba*$^{+/-}$, and *Manba*$^{-/-}$ mice 3 days after sham or cisplatin injection. **(E)** Representative Western blots of fibronectin and α-SMA of kidney tissues of wild-type and *Manba*$^{-/-}$ mice 3 days after sham or cisplatin injection (n = 3 per group). Densitometry analysis was performed to quantify protein expression. Data are means ± SEM. Statistical analysis by (A) Kruskal-Wallis followed by Conover-Iman test with Bonferroni adjustment, n=4 to 9 animals per group, #, P<0.0001, control group versus corresponding cisplatin group. ****P < 0.0001; **(B to D)**

Two-way ANOVA test, n=4 to 9 animals per group, &, $P<0.01$, $, $P<0.001$, #, $P<0.0001$, control group versus corresponding cisplatin group. *$P < 0.05$, **$P < 0.01$, ***$P < 0.001$, ****$P < 0.0001$; **(E)** One-way ANOVA with Tukey's post-hoc test. *$P < 0.05$, **$P < 0.01$, ***$P < 0.001$.

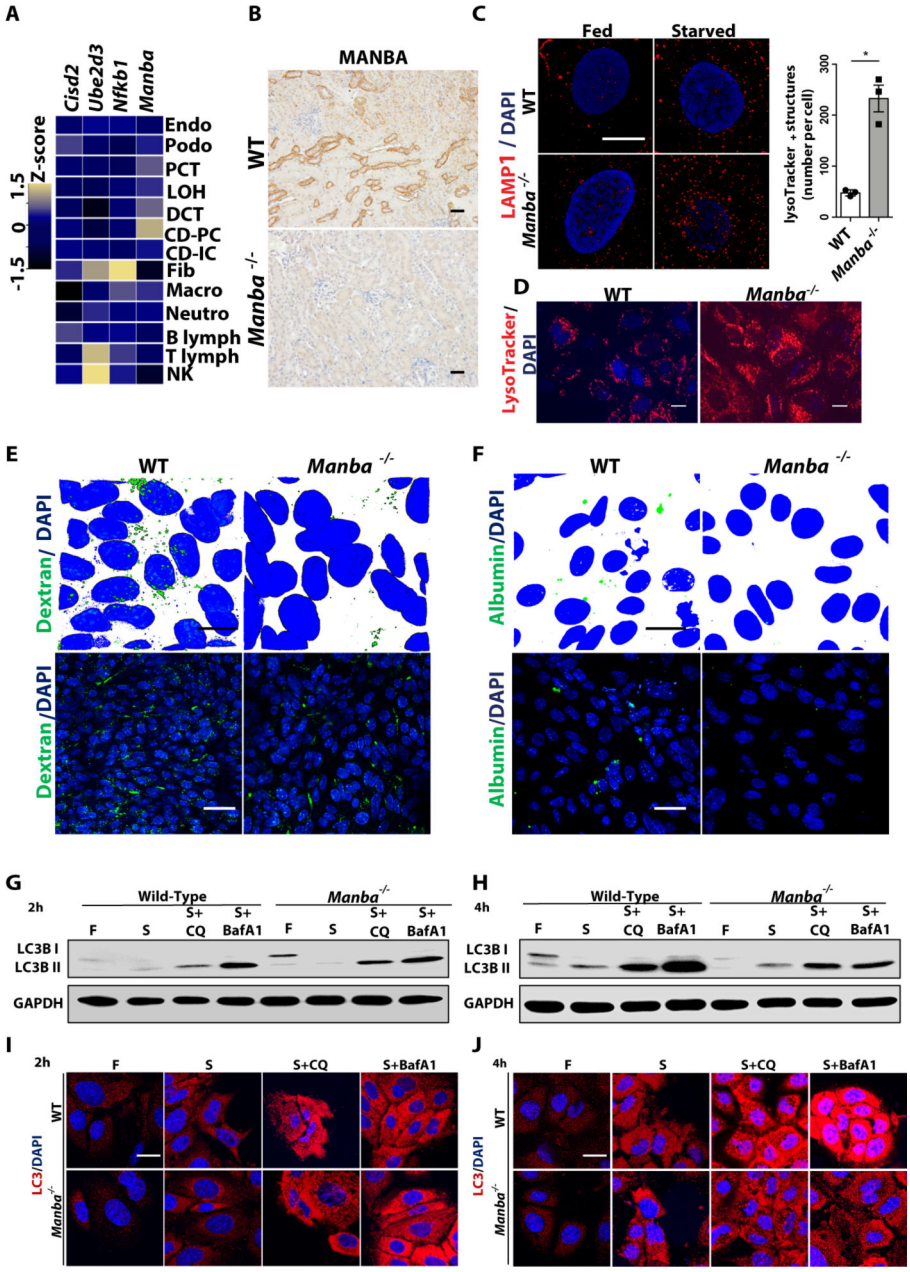

Fig. 4. *Manba* deficiency induces structural and functional lysosomal changes and blocks autophagy and endocytosis in cultured kidney tubule cells.

(A) Expression of *Manba, Nfkb1, Ube2d3*, and *Cisd2* in mouse kidney single cells (18). Blue/yellow corresponds to the gene expression Z-score. Endo, containing endothelial, vascular; Podo, podocyte; PCT, proximal convoluted tubule; LOH, loop of Henle; DCT, distal convoluted tubule; CD-PC, collecting duct principal cell; CD-IC, collecting duct intercalated cell; Fib, fibroblast; Macro, macrophage; Neutro, neutrophil; B lymph, B lymphocyte; T lymph, T lymphocyte; NK, natural killer cell. **(B)** Representative images of MANBA immunohistochemistry staining of control and *Manba* knock-out mouse kidney samples. **(C)** Representative confocal and 3D reconstruction images of TECs from wild-type and *Manba*$^{-/-}$ mice in fed or starved medium labeled with LAMP1 (red) and DAPI (blue).

(D) Representative images of kidney cells from wild-type and *Manba*$^{-/-}$ mice stained with Lysotracker (red) and DAPI (blue). Quantification of numbers of Lysotracker+ structures per cell. *$P < 0.05$, t test. **(E and F)** Representative confocal and 3D reconstruction images of TECs from wild-type and *Manba*$^{-/-}$ mice incubated with 10 kD Dextran labelled with Alexa-488 for 24h and 488-Alexa conjugated albumin for 4h, respectively. **(G and H)** Representative Western blots of LC3B protein expression in wild-type and *Manba* knockout cultured renal tubule cells in fed or starved medium with or without 50μM chloroquine (CQ) or 50 nM BafilomycinA1(BafA1) for 2h or 4h. **(I and J)** LC3B immunofluorescence staining of wild-type and *Manba*$^{-/-}$ tubule cells (LC3B [red] and DAPI [blue]) in fed or starved medium with or without 50μM chloroquine (CQ) or 50 nM BafilomycinA1(BafA1) for 2h or 4h. (B) Scale bar, 20 μm; (C to F and I to J) Scale bars, 10 μm.

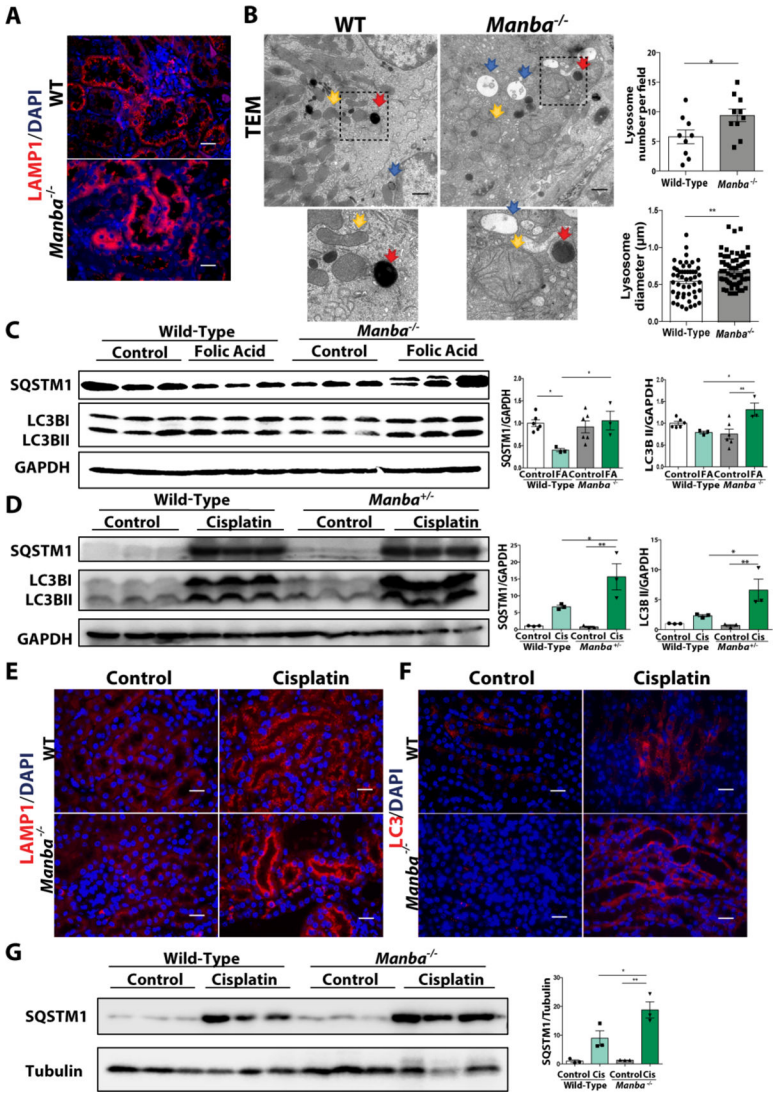

Fig. 5. *Manba* deficiency leads to impaired autophagy flux.

(A) Representative images of LAMP1 immunostaining of kidney sections of wild-type and *Manba*$^{-/-}$ aging mice. **(B)** Representative electron microscopic images showing lysosomes in wild-type and *Manba*$^{-/-}$ aging mice. Quantification of numbers and size of lysosomes in tubular epithelial cells of aging wild-type and *Manba*$^{-/-}$ mice. Black squares contain images at higher magnification. Yellow arrowhead indicates mitochondria; red, lysosomes; blue, autophagic vacuoles. **(C)** Representative Western blots of SQSTM1 and LC3B from kidney tissues of wild-type and *Manba*$^{-/-}$ mice 7 days after sham or folic acid (FA) injection (n = 3 to 6 animals per group). **(D)** Representative Western blots of SQSTM1 and LC3B from kidney tissues of wild-type and *Manba*$^{+/-}$ mice 3 days after sham or cisplatin injection (n = 3 per group). **(E and F)** Representative images of LAMP1 and LC3B immunostaining of kidney sections from wild-type and *Manba*$^{-/-}$ mice 3 days after sham or cisplatin injection (LAMP1 (red), LC3B(red) and DAPI (blue)). **(G)** Representative Western blots of SQSTM1 from kidney tissues of wild-type and *Manba*$^{-/-}$ mice 3 days after sham or cisplatin injection (n = 3 per group). Densitometry analysis was performed to quantify protein expression. Data

shown are means ± SEM. Y-axes differ between barplots. Statistical analysis by (B) t test, (C, D and G) One-way ANOVA–Tukey's post hoc test. *$P < 0.05$, **$P < 0.01$. (B) scale bar, 1μm; (A, E and F) Scale bars, 10 μm.

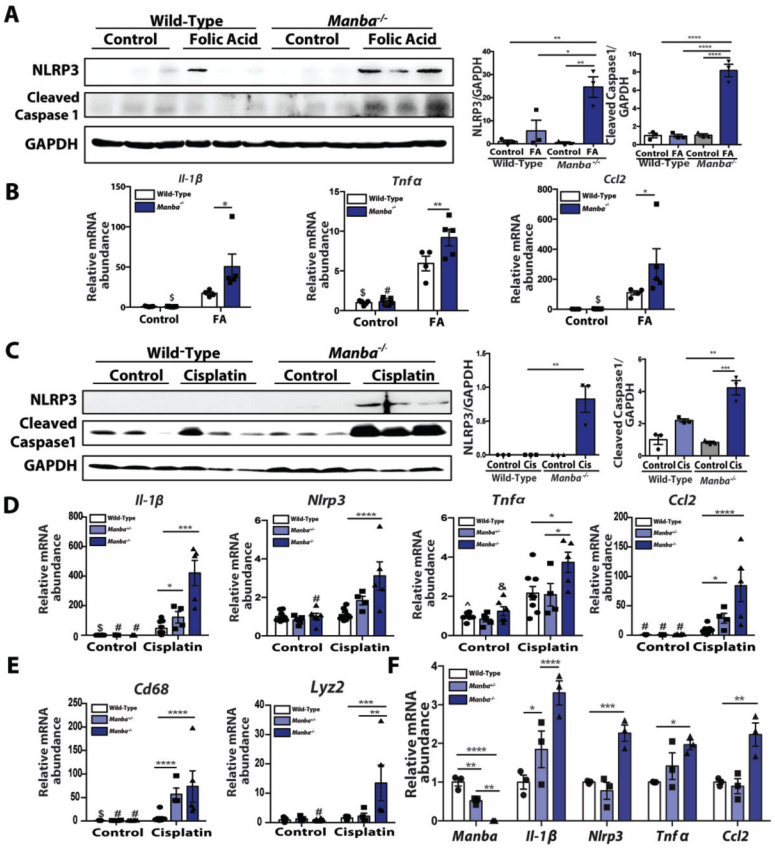

Fig. 6. Genetic *Manba* loss induces NLRP3 inflammasome signaling.

(A) Representative Western blots of NLRP3 and Cleaved Caspase1 from kidney tissues of wild-type and *Manba*$^{-/-}$ mice 7 days after sham or folic acid (FA) injection (n = 3 per group). **(B)** Relative mRNA abundance of *Il1β*, *Tnfα, Ccl2* in kidneys of wild-type and *Manba*$^{-/-}$ mice 7 days after sham or FA injection (n=4 to 7 animals per group). **(C)** Representative Western blots of NLRP3 and Cleaved Caspase1 in kidneys of wild-type and *Manba*$^{-/-}$ mice 3 days after sham or cisplatin injection (n = 3 per group). **(D and E)** Relative mRNA abundance of *Il1β*, *Nlrp3, Tnfα, Ccl2, Cd68* and *Lyz2* in wild-type, *Manba*$^{+/-}$, *Manba*$^{-/-}$ mice kidneys 3 days after sham or cisplatin. (n=4 to 9 animals per group). **(F)** Relative mRNA abundance of *Manba, Il1β*, *Nlrp3, Tnfα, Ccl2 of* wild-type, *Manba*$^{+/-}$, *Manba*$^{-/-}$ tubular epithelial cell. (n=3 per group). Densitometry analysis was performed to quantify protein expression. Data shown are means ± SEM. Statistical analysis by (A and C) One-way ANOVA–Tukey's post hoc test. *$P < 0.05$, ** $P < 0.01$, *** $P < 0.001$, **** $P < 0.0001$; (B and D to F) Two-way ANOVA test, ^, $P<0.05$, &, $P<0.01$, $, $P<0.001$, #, $P<0.0001$, control group versus corresponding cisplatin group. * $P<0.05$, ** $P<0.01$, *** $P<0.001$, **** $P< 0.0001$.

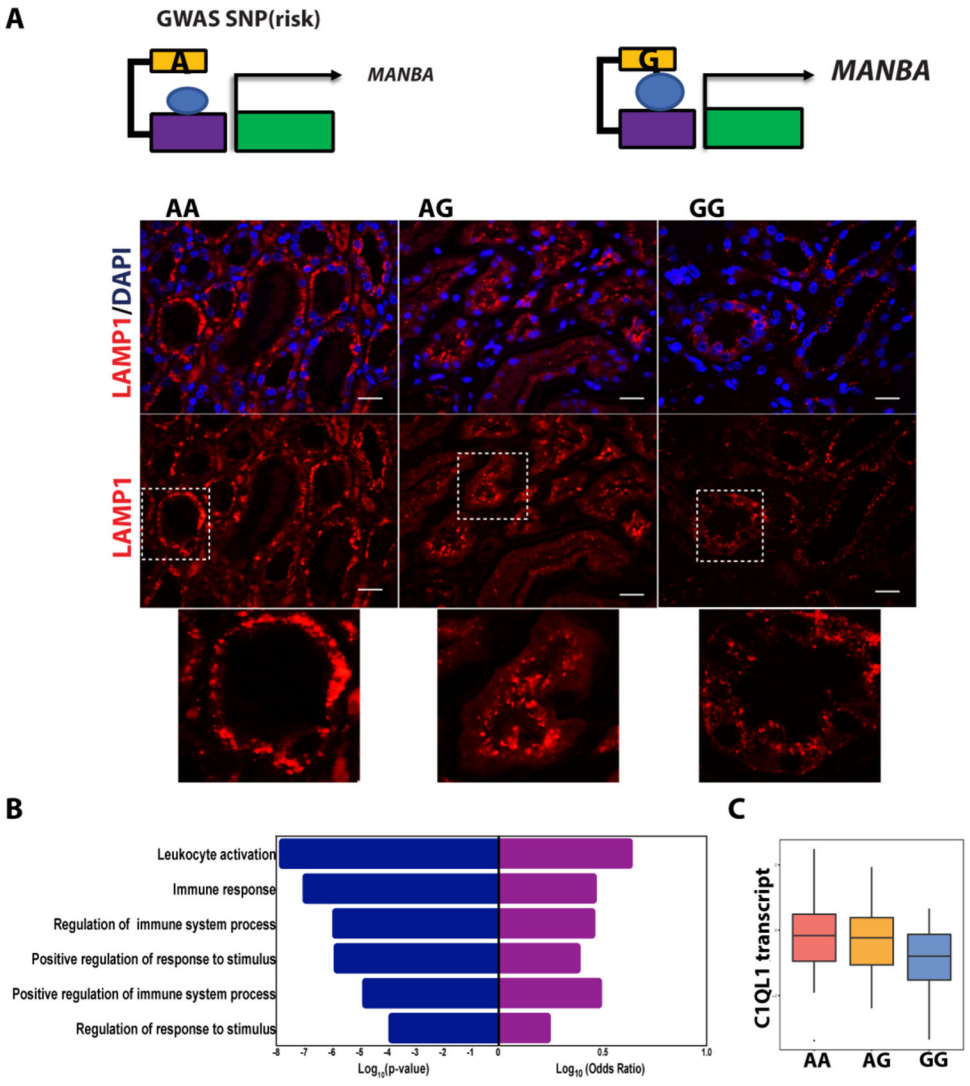

Fig. 7. Phenotypic characterization of kidneys obtained from subjects with CKD associated genetic-risk variants

(A) Representative images of LAMP1 staining in human kidney tissues of subjects with AA, AG and GG alleles, respectively. The A allele is the risk allele. White squares indicate images shown at higher magnification. Scale bar, 10 μm. **(B)** Gene expression analysis of microdissected kidney tubule samples from risk allele vs. reference allele. Pathway enrichment analysis (DAVID) of top differentially expressed genes. The bar plot shows the significance ($\log_{10}$(p) and $\log_{10}$(odds ratio)) of the enrichment of specific pathways. **(C)** Relative mRNA expression of *C1QL1* in reference and risk genotype kidney tubule samples.